Coulomb correlations in a two-dimensional electron gas in large magnetic fields

N. A. Fromer, C. Schüller, C. W. Lai, and D. S. Chemla
Department of Physics, University of California at Berkeley, Berkeley, California 94720
and Materials Sciences Division, Lawrence Berkeley National Laboratory, Berkeley, California 94720

I. E. Perakis
Department of Physics, University of Crete, P. O. Box 2208, 710 03, Heraklion, Crete, Greece

D. Driscoll and A. C. Gossard
Department of Electrical and Computer Engineering, University of California at Santa Barbara, Santa Barbara, California 93106
(Received 19 June 2002; published 13 November 2002)

We present an investigation of the dynamics of the inter-Landau-level (LL) excitations of a two-dimensional electron gas (2DEG) in large magnetic fields using coherent time-resolved nonlinear spectroscopy. The results are compared directly with measurements on undoped quantum wells. We observe time-dependent Coulomb coupling between the LL's induced by the 2DEG that induces a large transfer of oscillator strength to the lowest LL. The time dependence of the nonlinear response reveals non-Markovian and memory effects of the photoexcited system that cannot be understood in terms of the random phase approximation. We introduce a theoretical approach that treats the interactions of the magnetoexcitons with the 2DEG excitations and qualitatively accounts for the most salient experimental results in terms of shake-up of the 2DEG.

DOI: 10.1103/PhysRevB.66.205314 PACS number(s): 78.47.+p, 78.67.De, 73.20.Mf, 42.50.Md

I. INTRODUCTION

Correlation effects in photoexcited undoped semiconductors have been extensively investigated over the past decade.[1–4] Time-resolved coherent nonlinear spectroscopy experiments have given direct evidence of high-order Coulomb correlation processes whose description requires the revision of well-established theoretical treatments such as the random phase approximation (RPA),[5] Boltzmann kinetics,[6,1,7] and the thermal bath pictures of relaxation and dephasing.[1,8] Even the notion of weakly interacting ''quasiparticles,'' a cornerstone of condensed matter physics, must be revisited when describing the ultrafast nonlinear optical response of semiconductors.

So far, however, correlations in the ground state (full valence bands and empty conduction bands) are often neglected, although that state is strongly correlated.[9] Indeed most treatments assume that this ground state is rigid and just provides the band structure and the high frequency dielectric screening.[10] Such a viewpoint is based on the observation that the lowest excitations of the ground state electrons are high energy interband electron-hole (e-h) pair excitations, which can adjust almost instantaneously to the dynamics of the carriers photoexcited near the band gap.[9] This approximation holds well for undoped semiconductors, where therefore the only Coulomb correlations that need to be considered are dynamically generated by the optical excitation.[11] In that case the most widely used theoretical approach for describing the optical response is the dynamically controlled truncation scheme (DCTS).[12–14] In this theory, the response of the semiconductor is expanded in terms of the number of created e-h pairs and consistently truncated. This can be accomplished because of the correspondence between the number of photoexcited e-h pairs in the system and the sequence of photon absorption and emission. In this way it is possible to systematically include all correlations that contribute to a specified order in the applied field.

Clearly, the almost unexplored dynamics of strongly correlated systems, whose ground state electrons interact unadiabatically with the photoexcited e-h pairs, raises very fundamental issues. This is the case for modulation-doped quantum wells (MDQW's), where a two-dimensional electron gas (2DEG) exists in the sample prior to optical excitation and can react to photons and photoexcited carriers. In particular, with carriers present in the system before excitation, the correspondence between photoexcited e-h pairs and photon absorption/emission breaks down and the DCTS fails.

Previous efforts have developed a formalism able to handle the case where correlation with with a photoexcited electron-hole plasma[15] or an electron Fermi sea (FS) dominates the coherent optical response.[16] If the electron FS can respond to the photoexcited e-h pairs in time scales shorter than the pulse duration, it behaves to first approximation as a thermal bath, and can be treated within the dephasing and relaxation time approximations.[17–19] This picture becomes more complicated when a magnetic field is applied. The conduction and valence bands break down into Landau levels (LL), the kinetic energy is quenched, and the Coulomb interaction effects are enhanced.[20,21] The 2DEG enters the quantum Hall effect (QHE) regime[22,23] and supports low energy, intra-LL, and inter-LL excitations[24,25] whose times scale are comparable to or longer than the measurement times. When such slow degrees of freedom are coupled to the photocarriers the Boltzmann semiclassical picture of collision localized in time and space breaks down, and quantum mechanical interference effects dominate the interaction process. This is the case even for electron-phonon coupling where the noninstantaneous phonon response leads to non-Markovian

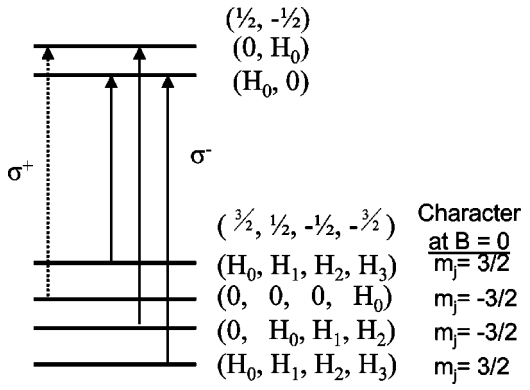

FIG. 1. Selection rules for optical transitions in a magnetic field. Transitions can only be made to the lowest electron level, with harmonic oscillator index 0, from a valence band state with the same $n=0$ character, and must also satisfy the change in angular momentum $\Delta m_J = \pm 1$.

memory effects readily observed in the ultrafast nonlinear optical dynamics.[1,6,8] The presence of the 2DEG intra-LL and inter-LL excitations raises yet another difficulty since they consist of electrons and thus are indistinguishable from the photoexcited carriers. In this case, one needs to account for the *coupled* time evolution of photoexcited *e-h*/2DEG system. Recently, what is believed to be the first experimental studies of the role of collective intra-LL excitations in the ultrafast nonlinear optical dynamics of the 2DEG were reported.[26,28]

We present here an investigation of the dynamics of the 2DEG inter-LL excitations, using time resolved nonlinear spectroscopy. The 2DEG electrons can screen the Coulomb interactions so that the Hartree-Fock (HF) interactions between excitons[27] (*X*) become much less important in describing the response of the system. However, the interactions between the photoexcited *X* and the 2DEG have other strong effects. The presence of low energy excitations of the 2DEG create the possibility of additional scattering channels through which the photoexcited electrons can relax.[28] Such scattering, described below in more detail, has much less effect on carriers excited to the lowest available level LL (LL0) while it can significantly affect the carriers excited to higher LL's. Also, the collective excitations of the electron gas are long-lived objects themselves. The inter-Landau-level excitations, i.e., the magnetoplasmons[29–31] (MP) evolve in time according to their own energy and dephasing and can interact with the photoexcited carriers. These interactions lead to memory effects in the time evolution of the photoexcited system, which affect the time-dependence of the nonlinear response. These effects will be explained in detail below, as we interpret our experimental results. We observe strong, time-dependent Coulomb coupling between the LL's induced by the 2DEG that enhances the LL0 signal. The latter shows unusual behavior as a function of time delay, which cannot be understood in terms of the RPA. These results are compared directly with measurements on undoped quantum wells (QW's). We also introduce a theoretical approach that treats the interactions of the magnetoexcitons with the 2DEG excitations and qualitatively accounts for the most salient experimental results.

The paper is organized as follows, in Sec. II we discuss the linear optical response of the MDQW samples, which characterize the sample and also demonstrate some of the effects of the *X*-2DEG interactions we are studying. In Sec. III we present the nonlinear response of a MDQW sample, compared directly with an undoped QW sample. This will illustrate the strong time-dependent Coulomb coupling caused by the presence of the 2DEG in the MDQW sample. In Sec. IV we present a model based on a microscopic theory for describing a general system with ground state correlations, and show that we are capable of simulating our experimental results. We are able to show that the unusual nonlinear optical response of the MDQW sample comes from the interaction between photoexcited carriers and inter-LL excitation of the 2DEG.

II. LINEAR OPTICS

Before discussing the nonlinear optical response of our system, it is useful to examine the linear optics. This will help expose some of the interaction effects caused by the presence of the 2DEG. The sample studied here was a MDQW, whose active region consists of 10 periods of a 12 nm GaAs well and a 42 nm $Al_{0.3}Ga_{0.7}As$ barrier, the central

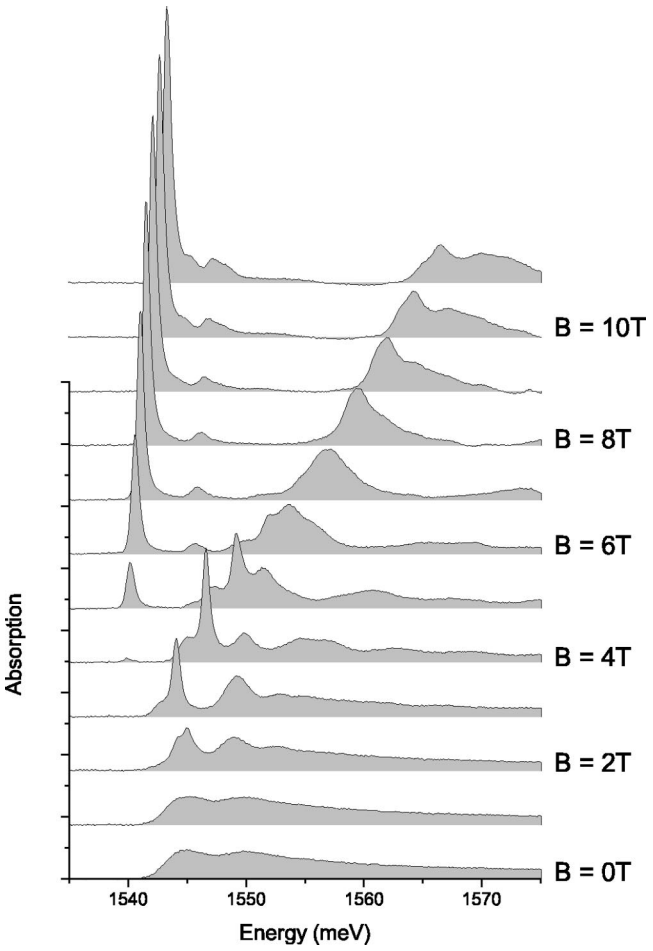

FIG. 2. Absorption spectra of a MDQW sample in a magnetic field.

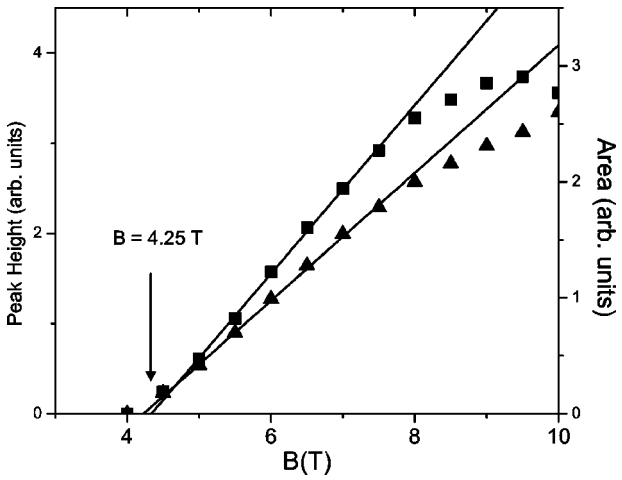

FIG. 3. LL0 absorption peak height and area in a magnetic field for the MDQW sample. Triangles are the peak area; squares the peak height. Both extrapolate to zero at ~4.3 T, giving a measurement of the density of doped electrons of 2.1×10^{11} cm^{-2}.

12 nm doped with Si, which was antireflection coated and mounted on sapphire windows for transmission measurements. The carrier density under illumination is $n=2.1\times10^{11}$ cm^{-2}. The sample has a low temperature mobility of $\mu\approx10^5$ cm^2/V s. The sample was immersed in superfluid helium in an magneto-optic cryostat, at a temperature of 1.7 K. The linear absorption measurements were taken using a broad band incoherent light source at low intensity.

The band structure of GaAs is well described by the effective mass approximation. The dipole allowed optical transitions from the four heavy and light hole (hh and lh) bands to the conduction band in GaAs QW's are induced by circularly polarized photons ($\sigma^{\pm}$). The addition of a magnetic field lifts the degeneracy between the spin-up and spin-down conduction band states, as well as splitting the conduction band into a series of degenerate Landau levels. The dependence of the valence band structure on the magnetic field is complex, due to strong band mixing.[32–34] The eigenvectors for the valence band states take on the four-component spinor form $(F_{3/2,n-2},F_{1/2,n-1},F_{-1/2,n},F_{-3/2,n+1})$, where the first subscript is the z component of the angular momentum m_J, and the second is the harmonic oscillator index, which describes the nature of the Landau level associated with that m_J state. The selection rules require the photon can only couple states that have the same harmonic oscillator character n. For excitations into the lowest conduction band Landau levels, $n=0$, the lowest energy transitions are shown in Fig. 1. These transitions were calculated to be the lowest in energy for GaAs QW's in high field.[34] As Fig. 1 shows, there are several transitions to both of the lowest electron Landau levels excited by σ^- polarized light, and only one transition excited by σ^+. Because of this difference, we have performed our nonlinear experiments using σ^+ polarized light, to simplify the interpretation.

Even without the Coulomb interaction, the presence of the doped conduction band electrons changes the linear optics of the QW. The extra electrons in the lower Landau levels prevent the addition of electrons because of the Pauli exclusion principle. The filling factor is defined as $\nu=N_e/D=2\pi l_c^2 N_e\propto 1/B$. At some field, all the electrons can fit into the lowest Landau level, with all the others empty ($\nu=1$). It is only once we reach this point that we should be able to see absorption into the lowest Landau level. This can be seen in Fig. 2, which shows the linear absorption spectra of a MDQW sample for many different magnetic fields. Looking at Fig. 2, we can see the onset of absorption into the lowest Landau level, LL0, between $B=4$ T and $B=5$ T. Figure 3 gives more details of this effect, by looking at the peak height and area of LL0 as a function of the field. By extrapolating the LL0 peak height or area down to zero, we can confirm the doped carrier density. For our sample, the peak height and area reach zero at $B\sim4.3$ T, which confirms our electron density to be $n\approx2.1\times10^{11}$ cm^{-2}.

Let us examine the linewidths of the Landau level peaks. Figure 4 shows the peak energy and linewidths of the lowest two Landau levels of the MDQW sample. While the linewidth of LL0 is approximately constant, the linewidth of LL1 increases significantly once LL0 starts to appear in the spectrum. This is an important point to notice: when the LL0 transition has finite oscillator strength, the LL1 peak is broadened significantly. The hh LL0 peak is comparable in width to what is seen in undoped QW samples, and is fairly well fitted by a single Lorentzian line. However, in an undoped QW sample, the linewidth of LL1 also remains more or less constant, and does not become significantly larger than that of LL0.

The increase in the LL1 linewidth for smaller filling factors implies an increase in the dephasing rate of this state due to scattering with the 2DEG, which for these fields is entirely

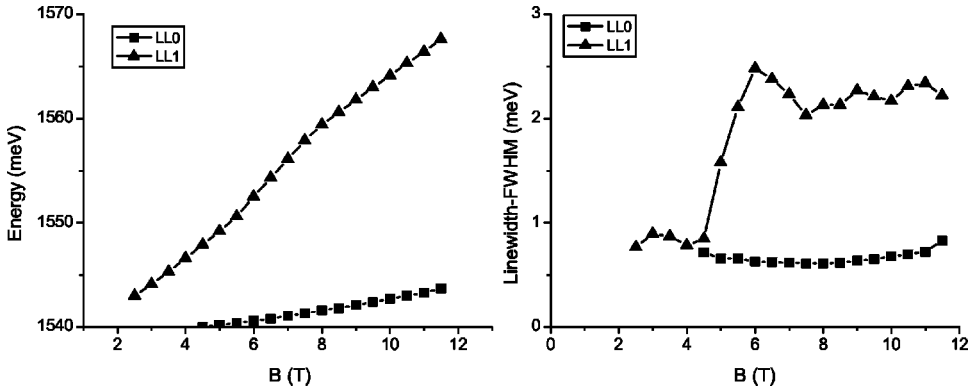

FIG. 4. Peak energy and linewidth vs magnetic field for the MDQW sample, for both the lowest (LL0) and next highest (LL1) Landau levels. Notice the sharp increase in the LL1 linewidth once LL0 starts to appear in the absorption spectrum.

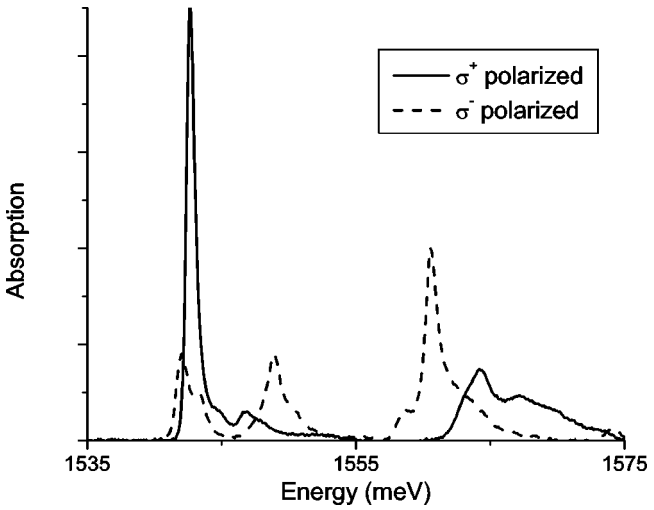

FIG. 5. Absorption spectra for the MDQW sample at $B=10$ T, both σ^+ (solid) and σ^- (dashed) polarized.

in LL0. The increased dephasing rate is a result of additional scattering mechanisms available for LL1 excitations due to the presence of the 2DEG. For instance, a LL1 *e-h* pair can scatter with the 2DEG and relax to a lower energy while exciting the electron gas. In fact, since the inter-LL excitations of the 2DEG, MPs, have an energy close to the inter-LL energy spacing, the scattering between a LL1 *e-h* pair and the 2DEG is nearly resonant, greatly enhancing this process. These scattering processes are described in more detail in Sec. IV.

We can also see here that the absorption spectra is different for σ^- polarized light. Figure 5 shows the absorption spectra at $B=10$ T for both the σ^+ and σ^- polarizations. The σ^- spectrum is more complicated, with a double-peaked lowest energy transition, and an additional light hole peak a bit higher in energy. These additional peaks make analysis of the four-wave mixing (FWM) signal more complicated, since the lowest peak actually represents several transitions to different spin states of the conduction band (see Fig. 1).

III. FOUR-WAVE MIXING RESULTS

In this section, we present an investigation of the nonlinear dynamics of the 2DEG inter-LL excitations. The nonlinear measurements were performed on the same MDQW sample discussed above in the linear absorption measurements. For most of the measurements in this study, the total number of carriers excited by the laser was kept below 2×10^{10} cm^{-2}, or $n/10$. We will discuss the dependence of our results on the excitation power later in the paper. Comparison measurements were made on an undoped QW sample with similar well and barrier sizes. We used two criteria for these comparisons, by adjusting the laser (i) to excite the same number of electron-hole pairs into each LL with a given laser pulse, or (ii) to produce the same FWM signal in the nonlinear susceptibility approximation, $S\propto|P^{(3)}|^2=|\chi^{(3)}|^2I_L^3$, where $P^{(3)}$ is the third-order polarization and I_L^3 the laser intensity. In our resonance conditions the third-order susceptibility is assumed (based on single-frequency calculations of the polarization) to be proportional to the square of the absorption coefficient, $\chi^{(3)}\approx(\chi^{(1)})^2\approx\mathrm{Im}[\chi^{(1)}]^2\approx\alpha^2(\omega)$.[28] The effects reported here were observed for comparisons using both criteria. We performed spectrally resolved four-wave mixing (SR-FWM) experiments, with a laser pulse duration of $100\leqslant\tau\leqslant200$ fs. The laser was tuned to excite varying proportions of the lowest LL (LL0) and the next highest LL (LL1), and the beams were σ^+ circularly polarized.

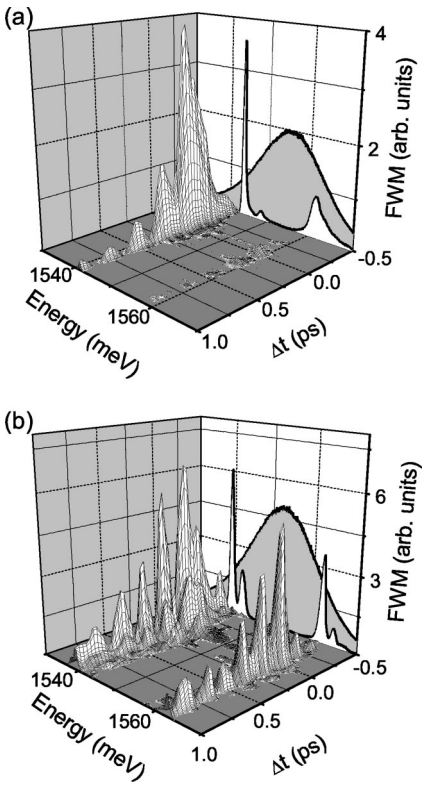

FIG. 6. Spectrally resolved FWM signal at $B=8$ T for excitation of an equal number of electron-hole pairs into both LL0 and LL1, for (a) the MDQW sample and (b) the undoped sample. The back screens show the laser and sample absorption spectra.

Typical SR-FWM signals, $S_{\mathrm{SR}}(\Delta t,\omega)$, for both the doped and undoped samples are shown in Fig. 6, with the laser tuned to excite both LL0 and LL1 equally (laser and sample absorption spectra are projected on the back panels). Several unusual features are immediately apparent in the signal from the doped sample, $S_{\mathrm{SR}}^{\mathrm{doped}}(\Delta t,\omega)$, Fig. 6(a). The most striking is that despite an equal excitation of both LL's, the MDQW shows a LL0 signal that is 35 times larger than the LL1 signal. Measurement of the undoped QW, $S_{\mathrm{SR}}^{\mathrm{undoped}}(\Delta t,\omega)$, Fig. 6(b), shows almost equal emission from both LL's, in proportion to the excitation. We see that the spectral distribution of the signal from the undoped sample approximately follows the mean-field HF theory,[27] but the signal from the MDQW sample is drastically different.

Also, although we see emission almost entirely from LL0, the signal has very pronounced beats as a function of Δt, with a period given by the inverse of the energy difference between LL0 and LL1. Such strong beating in Δt from only a single emission energy is a clear signal of non-Markovian

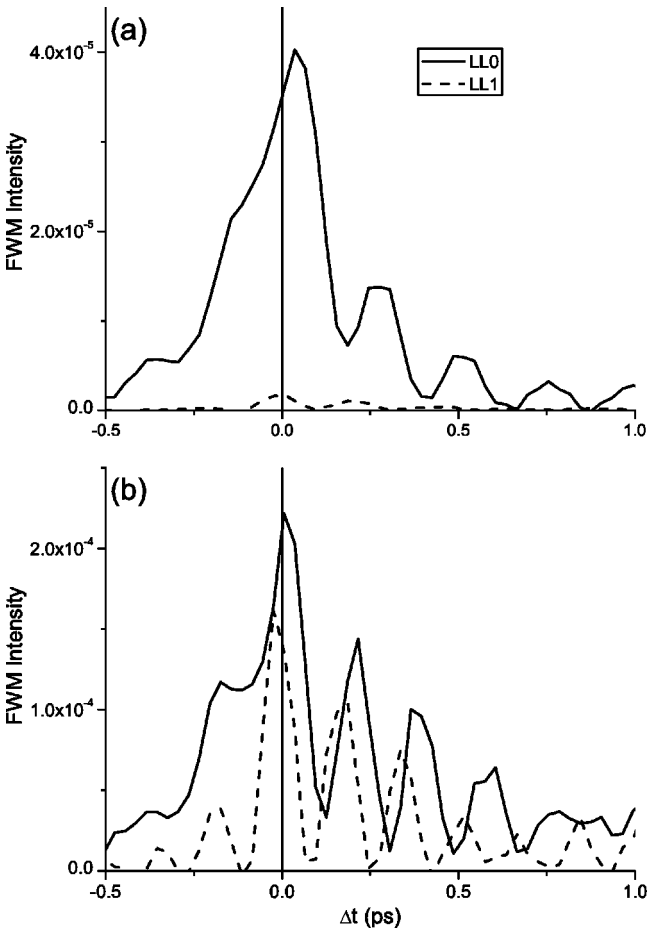

FIG. 7. FWM vs time delay for (a) the MDQW sample and (b) the undoped sample at $B=8$ T, from the LL0 and LL1 maxima. The solid curves are the signals from LL0, and the dashed curves are from LL1. The laser is tuned to excite both levels (LL0 and LL1) equally.

dynamics. Comparing this to the signal from the undoped QW, we see that $S_{\mathrm{SR}}^{\mathrm{undoped}}(\Delta t,\omega)$ also shows beats, but from both emission peaks, as expected from the HF theory. This is made clearer in Fig. 7, which shows the dependence of S_{SR} on Δt for two values of ω, corresponding to the maximum signal from LL0 and LL1, for both samples.

The picture is just as unusual when we tune the laser frequency to excite almost entirely into LL1, exciting 60 times the carriers into LL1 than into LL0. Figure 8 shows $S_{\mathrm{SR}}(\Delta t=0,\omega)$, the FWM spectra for $\Delta t=0$, for both samples under these excitation conditions. It is clear that the signal from LL0 is greatly enhanced relative to LL1 in the MDQW. In the undoped sample, there is almost no signal from LL0, as expected from the excitation (shown in the inset), while in the doped sample the LL0 signal is comparable to the LL1 signal. We can get an estimate for how large this enhanced LL0 signal is by comparing the relative emission of the two LL's with the excited carriers in each level. We define the relative emission ratio R as

$$R=\frac{S_m^{\mathrm{LL0}}/N_{\mathrm{LL0}}}{S_m^{\mathrm{LL1}}/N_{\mathrm{LL1}}}, \tag{1}$$

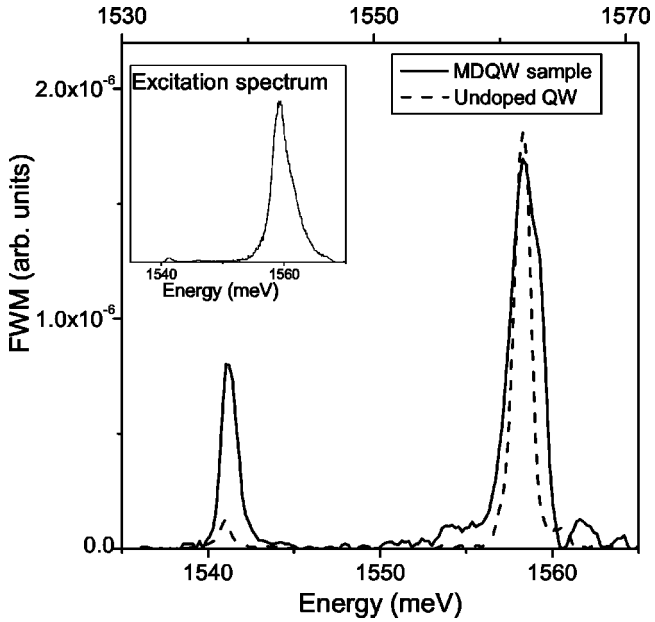

FIG. 8. SR-FWM signal at $B=8$ T, $\Delta t=0$ ps from both the MDQW sample (solid) and undoped sample (dashed). The inset shows the excitation density spectrum, giving a ratio of 60:1 excitation of LL1 over LL0. The energy scales are different for the two samples, with the lower energy scale for the MDQW sample.

where $S_m^{\mathrm{LL0(LL1)}}$ is the maximum signal emitted from LL0 (LL1), and $N_{\mathrm{LL0(LL1)}}$ is the number of photoexcited pairs in LL0 (LL1). If the emission is in direct proportion to the excitation, as we expect from the HF theory, then we should find $R=1$. $R>1$ means that the LL0 signal is larger than expected from the excitation, while $R<1$ means the LL0 signal is smaller than expected. For the signals shown in Fig. 8, we find that for the undoped sample $R^{\mathrm{undoped}}=1.3$, close to the expected $R=1$, while for the MDQW sample $R^{\mathrm{doped}}=17.5$, a huge enhancement compared to the undoped signal. Since the calculated excitation densities are estimates, the value of R is more of a guideline than a precise measure of the enhancement. However, a difference of more than an order of magnitude is an unambiguous demonstration of the effects of the 2DEG on the FWM signal.

In addition to the transfer of oscillator strength to LL0, $S_{\mathrm{SR}}^{\mathrm{doped}}(\Delta t,\omega)$ also shows a very unique dependence on Δt when we preferentially excite LL1. According to the HF theory for FWM in semiconductors, the rise time of the $\Delta t<0$ signal should be 1/2 the decay time for $\Delta t>0$, and this is the measured result for the undoped QW sample. This is also the measured result for the signal from LL1 in the MDQW, but surprisingly the signal from LL0 is almost symmetric as a function of Δt, with comparable signals for $\Delta t<0$ and $\Delta t>0$. Figure 9 shows the dependence of S_{SR} on Δt at the emission maxima of LL0 and LL1 for the MDQW sample. Such a large signal for $\Delta t<0$ can only be a result of correlation effects beyond the HF theory.[5] However, the effect is only seen in the signal from LL0, and only in the doped sample, which implies that in this case the correlations are induced by the presence of the 2DEG in the doped sample.

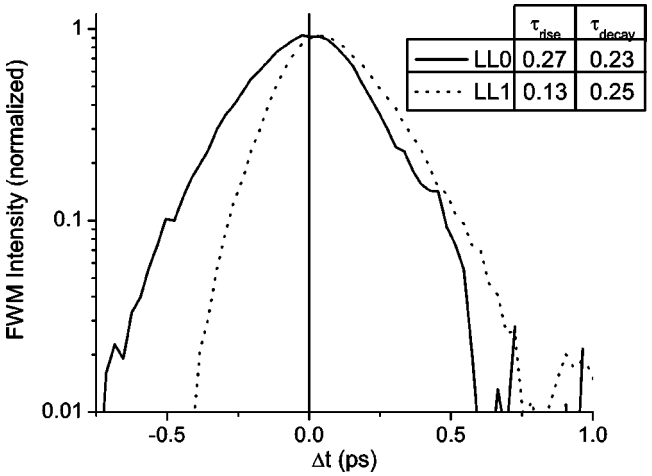

FIG. 9. FWM vs time delay Δt for the MDQW's, the MDQW sample, at $B=8$ T. The solid curve is the signal from LL0 and the dotted curve is from LL1. The laser is tuned to excite LL1 (60:1 over LL0), and the signals have been normalized for clarity. The decay time for both curves is ≈ 0.25 ps. The rise time for the LL1 signal is 0.13 ps, as expected from mean-field theory, while for LL0 it is 0.27 ps.

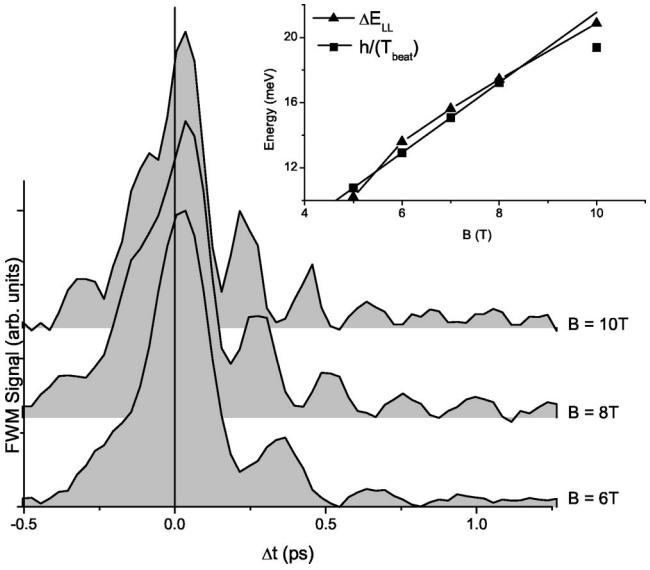

FIG. 10. FWM emission from LL0 vs time delay for the MDQW sample as a function of magnetic field, when the laser is tuned to excite both levels (LL0 and LL1) equally. The FWM curves are offset for clarity. The inset shows the comparison between the LL spacing measured in the absorption spectrum (in triangles) and the inverse of the beat period T_{beat} seen in the LL0 FWM signal vs Δt (in squares).

Since we are exciting several LL's in these experiments, we expect that the inter-LL excitations of the 2DEG, MP's, are important for understanding these results. The MP energy is close to the inter-LL magnetoexciton energy, so we must account for the almost resonant creation and destruction of the MP excitations nonperturbatively. In particular, it is possible for a photoexcited LL1 electron to scatter into LL0 while exciting the 2DEG. The scattering to this new state provides additional dephasing for the LL1 photoexcited carriers, which will affect the FWM signal. Since this scattering process is nearly resonant, it is also possible that during the time evolution of the excited system, some of the excitation energy is temporarily stored in the MP excitation, leading to memory effects in the FWM signal. This process, which is analogous to coherent anti-Stokes Raman scattering except with MP's instead of phonons,[35] is examined in more detail in the next section. There we will show that we must include these nearly resonant exciton-2DEG interactions in order to understand the unusual effects in the optical response of the MDQW that we are describing here.

For the remainder of this section, we will examine the dependence of the FWM signal from the MDQW sample on the magnetic field, the pulse duration, and the excitation power. These experiments will help us to understand the nature of the correlation effects we have described above for the MDQW sample in a large magnetic field.

By changing the magnetic field, we confirmed that the beat frequency seen in the signal from LL0 when we excite both levels changes with the cyclotron energy and is very close to the LL spacing. This is shown in Fig. 10, which shows $S_{\mathrm{SR}}^{\mathrm{doped}}(\Delta t)$ at the LL0 energy for $B=6$, 8, and 10 T when we excite both LL0 and LL1 equally. The inset shows good agreement between the inverse beat period (in meV) and the LL spacing at several magnetic fields.

Looking at the behavior of the signal from LL0 when we excite only into LL1, we see that the enhanced LL0 signal is only present for magnetic fields large enough that LL0 is partly empty (filling factor $\nu<2$ in the quantum Hall notation). Figure 11 shows $S_{\mathrm{SR}}^{\mathrm{doped}}$ vs Δt at the LL0 energy for $B=4$, 6, 8, and 10 T when we excite directly to LL1 only. For $B>4$ T, we see similar curves (including the large signal for $\Delta t<0$), but for $B=4$ T ($\nu>2$) there is only a much

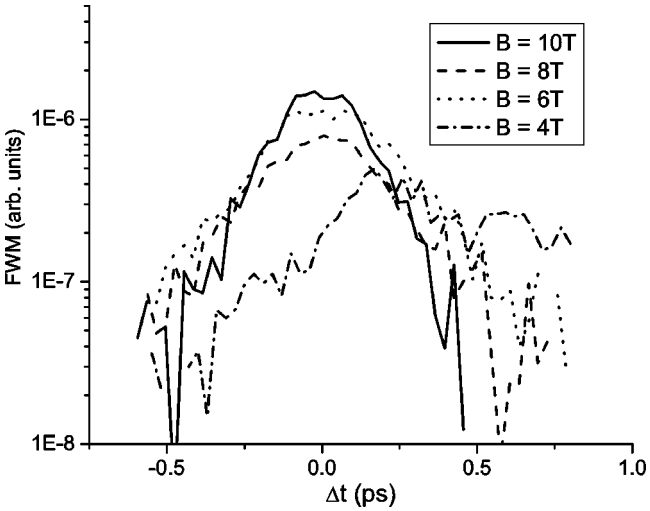

FIG. 11. FWM emission from LL0 vs time delay for the MDQW sample as a function of magnetic field, when the laser is tuned to excite only LL1 directly. For $B=4$ T ($\nu=2.18$), there is no off-resonant signal from LL0, but for higher fields (once there is available space in LL0), we see the strong off-resonant signal with the nearly symmetric time delay dependence. Note that a logarithmic scale is used.

weaker signal from LL0, and it does not have the symmetric time delay profile we see for the higher fields. We can infer that the enhancement of the LL0 signal only exists at magnetic fields for which there is available space in LL0 before the excitation.

By leaving the laser tuned directly to LL1, but varying the width of the exciting laser pulse in energy, we determined that the ''off-resonant'' signal from LL0 for that excitation requires a small direct excitation of the level. When the pulse was slightly narrowed so that only 1/100 of the carriers are excited into LL0 rather than the 1/60 in the data discussed above, the LL0 signal dropped by nearly a factor of 30. This is shown in Fig. 12, which shows the relative emission R^{doped} for the MDQW sample for several different pulsewidths, corresponding to a relative excitation of LL0 between 1/100 and 1/40. As the figure makes clear, the strength of the off-resonant signal dropped off suddenly as we made the pulse narrower and excited less and less of the lowest level. We can conclude that while the 2DEG strongly enhances the signal from LL0 relative to LL1, this enhancement can only be observed when there is a small excitation of LL0 as well.

Finally, we have also measured $S_{\mathrm{SR}}^{\mathrm{doped}}(\Delta t,\omega)$ and $S_{\mathrm{SR}}^{\mathrm{undoped}}(\Delta t,\omega)$ as a function of the incident power, varying the photocarrier density in the range $n/10\rightarrow n$, where n is the number of doped carriers in the MDQW, $n=2.1\times10^{11}$ carriers/cm^2, both when the laser preferentially excites LL1 (60:1 excitation ratio, as above), and when we excite both levels together.

When we excite only LL1 with the laser at low excitation power, we see the large ''off-resonant'' signal from LL0, which has a large negative time delay signal (nearly symmetric as a function of Δt; see Fig. 9). The evolution of this signal as the excitation power is increased is shown in Fig. 13. The LL0 emission begins to develop weak beats as a function of Δt, with a very pronounced minimum at $\Delta t=0$ [the beats can also be seen more clearly in the solid curve in Fig. 15(b)]. Notice that there is no real decrease in the signal for negative time delay.

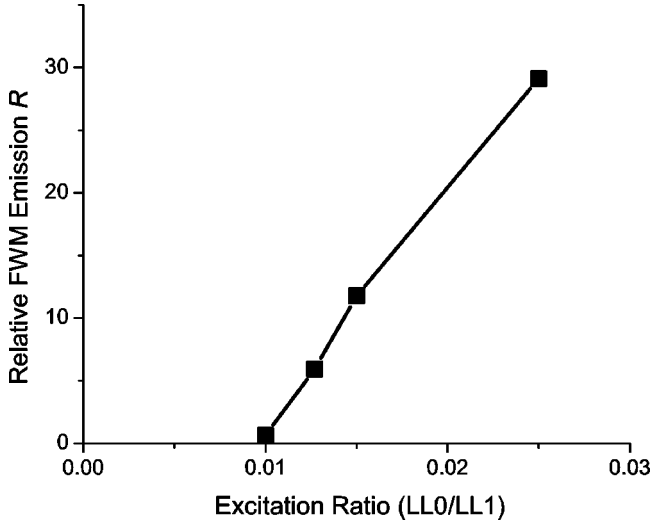

FIG. 12. Relative FWM emission R as a function of the relative excitation of LL0. For an excitation of 100:1 into LL1, there is no signal from LL0, but for excitation of 40:1, we see a very strong LL0 signal.

When we tune the laser to excite both LL0 and LL1, the LL0 signal exhibits pronounced beats in Δt at low power. As the power is increased, a large minimum at $\Delta t=0$ that is absent at low power begins to emerge. Figure 14 shows a comparison of the LL0 FWM emission at low power (excitation density $\approx n/10$) and at high power ($\approx n$) for this laser position.

In addition to these beats, the unusual transfer of oscillator strength from LL1 to LL0 seen in the MDQW sample is affected by the increase in power. To see this we calculate the relative emission ratio R, introduced above, for both samples as a function of the exciting laser power. We find that increasing the overall excitation power causes R^{doped} to begin to decrease towards unity, for either laser excitation. For example, $R^{\mathrm{doped}}=17.5$ in Fig. 8 at low power, and for the high excitation power it has decreased to $R^{\mathrm{doped}}\approx12$. We have also measured the power dependence of R^{undoped} from the undoped sample, and found, surprisingly, the opposite effect, that high excitation density *increases* the relative size of the LL0 signal (from $R^{\mathrm{undoped}}=1.3$ at low power to $R^{\mathrm{undoped}}\approx4.5$ at high power). While the difference between the R^{doped} and R^{undoped} is still large (approximately a factor of 3) at our highest measured power (excitation density $\sim n$), it has decreased from the order of magnitude enhancement seen at low power.

These changes as a function of increasing excitation density are such that the doped and undoped samples begin to look more similar in their overall nonlinear optical response. This is illustrated in Fig. 15, which shows the signal from both samples C and D at both the low and high excitation powers. While the two samples look quite different at low density, the curves start to appear more similar at the higher density. This can be understood qualitatively, since as the density of photoexcited carriers approaches that of the electron gas, the mean-field exciton-exciton interactions of the HF theory begin to dominate over the signal due to exciton-2DEG correlations. However, the $\Delta t=0$ dip in LL0 for the doped case is always larger than any beat seen in undoped sample, and at least for the excitation densities we have measured, the negative time delay signal for the undoped QW sample is always less than the positive delay signal, while the negative time delay signal in the doped sample seems to remain as large as the positive time delay signal.

IV. INTERPRETATION

To help understand the differences between the MDQW system and an undoped semiconductor, we will begin with a discussion of the qualitative structure of the Hilbert space of the system. From now on we will denote a general excited configuration of the electron gas by 2DEG*. The photoexcitations of the undoped system, or of the MDQW with the 2DEG at rest, consist of $1e$-h,$2e$-h, . . . ,le-h pair states created in the different LL's. Similarly, the Hilbert space of the 2DEG (with no photoexcited carriers) contains 1-MP,2-MP, . . . ,n-MP, . . . states. For the magnetic fields

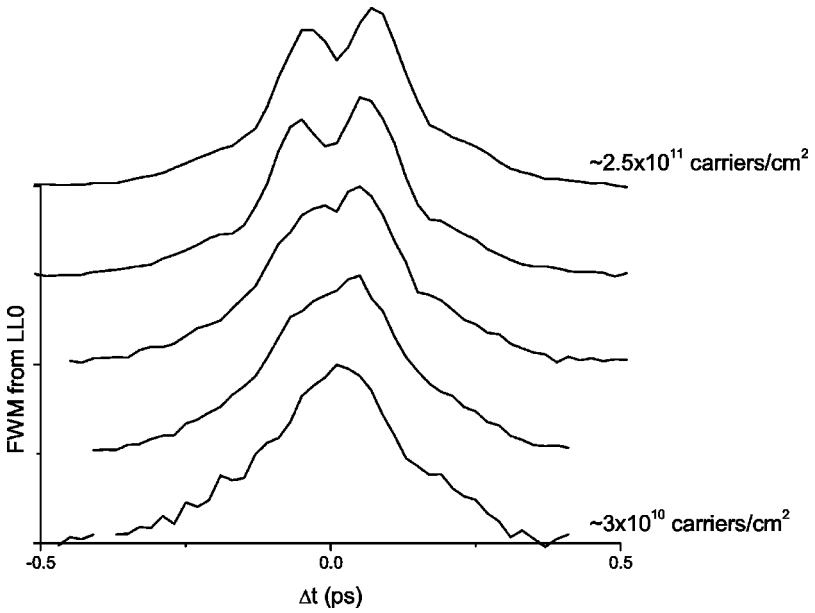

FIG. 13. FWM emission from LL0 vs time delay for the MDQW sample as a function of excitation density, at $B=10$ T, with only LL1 directly excited by the laser. The FWM curves are offset for clarity. As the excitation density is increased from $\approx n/10 \rightarrow n$, where n is the number of doped carriers in the MDQW, we see the development of beats in the signal, with a pronounced minimum at $\Delta t=0$.

of interest in our experiments, the ground state $|0\rangle$ has all the e-LLn and h-LLn empty, except the e-LL0, which contains the 2DEG at rest. However, the total Hilbert space, $\mathcal{H}_{\rm tot}$, contains many other 0-h states that can be photoexcited via nonlinear optical processes assisted by inelastic Coulomb scattering. Also, QW states that cannot be optically excited in the absence of X-2DEG interactions (due to optical selection rules) do contribute to $\mathcal{H}_{\rm tot}$, e.g., states with a MP and e and h not in LL's with the same indices. An example is the four-particle excitation $\{1\text{-MP}+1\text{-LL0-}e+1\text{-LL1-}h\}$. Such a state can result from the scattering of a LL1-e-h pair with the 2DEG and plays an important role in the optical properties of the MDQW. For simplicity, we will call these states, into which a photoexcited X can scatter, Y states.

The Y states describe new $\{1e\text{-}h+1\text{MP}\}$ four-particle excitations. Let us illustrate their meaning and origin by an example that is important for our experiments, starting with a LL1 exciton. The LL1 electron can scatter down to LL0 by emitting a MP. Since the MP energy is close to the e-LL0 $\rightarrow e$-LL1 energy spacing, the above interaction process is nearly resonant. It therefore provides an efficient decay channel of the LL1 exciton to a $\{1\text{-MP}+1\text{-LL0-}e+1\text{-LL1-}h\}$ four-particle Y excitation. Such a scattering process can occur for a LL0 X as well, but this process would be nonresonant, and therefore the decay of the LL0 X is suppressed as compared to that of the LL1 X. The scattering described above is a new interaction process between the photoexcited X states and the 2DEG, which provides additional dephasing of our system.[36] This dephasing is also non-Markovian, i.e., the processes are not instantaneous, producing a memory kernel in the time domain.

In Ref. 36, a detailed theory for describing a general system with strong ground state correlations is described. To connect with the experiments, we can derive a model based on this microscopic theory, but simplified to clarify the main physical ideas involved. Such ''average polarization models'' have greatly aided in understanding the many-body processes responsible for the FWM signal in undoped semiconductors.[5,37] We will consider only the two LL's excited in the experiments, LL0 and LL1, which will leave only a small set of coupled equations, depending on only a few parameters and simple enough to be integrated numerically on a PC. This will allow us to describe the dynamics due to the main physical processes in a straightforward way. We note that the qualitative features of the dynamics are robust and do not depend sensitively on our assumptions about the different interaction parameters.

The coupled first order polarization equations are

$$i\partial_t P_0^L(t)=(\Omega_0-i\Gamma_0)P_0^L(t)-V_{01}P_1^L(t)-W\overline{P^L}(t)-\mu\mathcal{E}(t), \tag{2}$$

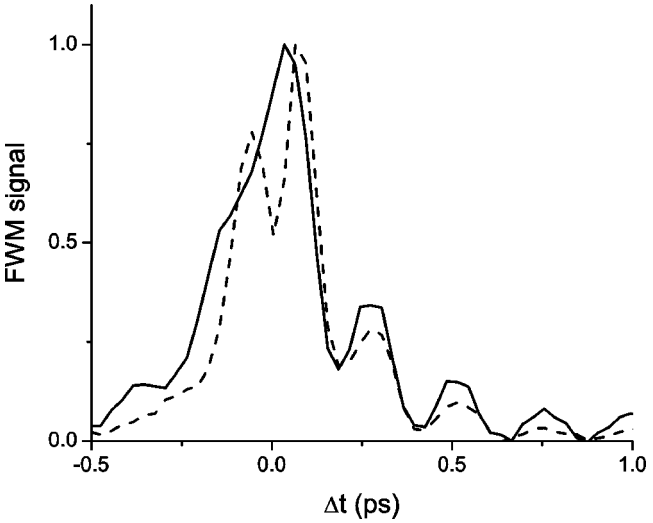

FIG. 14. FWM emission from LL0 vs time delay for the MDQW sample as a function of excitation density, at $B=8$ T, when both LL0 and LL1 are directly excited by the laser. The FWM curves are normalized for comparison. As the excitation density is increased from $\approx n/10 \rightarrow n$, we see the development of a pronounced minimum at $\Delta t=0$.

$$i\partial_t P_1^L(t) = (\Omega_1 - i\Gamma_1)P_1^L(t) - V_{10}P_0^L(t) + W\overline{P^L}(t) - \mu\mathcal{E}(t), \tag{3}$$

$$i\partial_t \overline{P^L}(t) = (\overline{\Omega} - i\gamma)\overline{P^L}(t) + [P_1^L(t) - P_0^L(t)]. \tag{4}$$

These equations describe the first-order response of the sample to the electric field pulse of the laser, $\mathcal{E}(t)$. The linear polarization $P_n^L(t)$ oscillates in time like a harmonic oscillator, with frequency Ω_n, damped by a phonon-induced dephasing rate Γ_n, and driven by the electric field of the exciting laser. These are the first and last terms, respectively, in Eqs. (2) and (3). The parameter $V_{01} = V_{10}^*$ describes the LL coupling of Ref. 27. We expect that the screening caused by the doped electrons in the 2DEG should lower the value of this coupling parameter for the MDQW case. The function $\overline{P^L}(t)$ describes the dephasing of the linear polarization $P^L(t)$ through the $X \leftrightarrow Y$ scattering process described above. It evolves in time according to its own energy $\overline{\Omega} \sim \Omega_0 + \Omega_M \sim \Omega_1$, and has a dephasing rate γ that accounts approximately for all of the states into which a Y excitation can scatter. The coupling parameter W gives the probability amplitude of the $X \leftrightarrow Y$ scattering process which drives $\overline{P^L}(t)$.

It is important to note that the dephasing of the optical polarization obtained within this model is non-Markovian. This can be clearly seen at the linear polarization level. We can solve Eqs. (2)–(4) analytically by Fourier transform:

$$[\omega - \Omega_n(\omega)]P_n^L(\omega) + V_{nn'}(\omega)P_{n'}^L(\omega) = -\mu\mathcal{E}(\omega)N_n^{1/2}, \tag{5}$$

where $n, n' = 0,1$ and $n \neq n'$. The exciton energy $\Omega_n(\omega)$ and the LL coupling $V_{nn'}(\omega)$ now include frequency-dependent self-energy corrections due to the X-2DEG scattering,

$$\Omega_n(\omega) = \Omega_n + \frac{W}{\omega - \overline{\Omega} + i\gamma} - i\Gamma_n \tag{6}$$

and

$$V_{nn'}(\omega) = V_{nn'} + \frac{W}{\omega - \overline{\Omega} + i\gamma}. \tag{7}$$

The frequency dependence of the above magnetoexciton energies and coupling constants is a manifestation of the non-Markovian behavior of the system. This arises because part of the optical excitation is temporarily stored in the shake-up

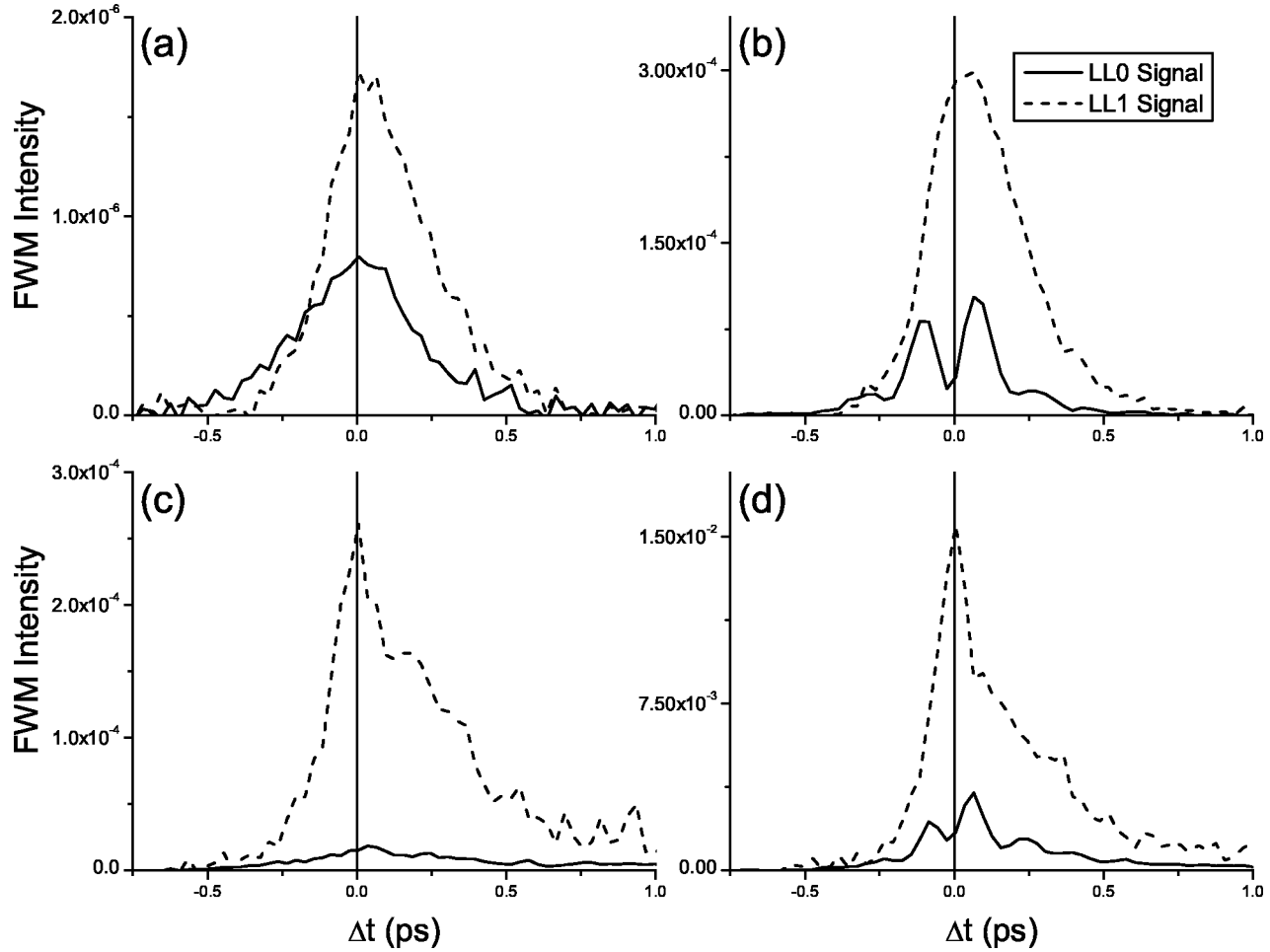

FIG. 15. FWM vs time delay for at $B = 8$ T, from the LL0 and LL1 maxima. The solid curves are the signals from LL0, and the dashed curves are from LL1. The laser is tuned to excite LL1 preferentially (60:1). The panels show the signals (a) from the MDQW sample at low density ($\approx n/10$), (b) from the MDQW sample at high density ($\approx n$), (c) from the undoped sample at low density, and (d) from the undoped sample at high density. There is a qualitative similarity between (b) and (d) at high density, despite the large differences in (a) and (c).

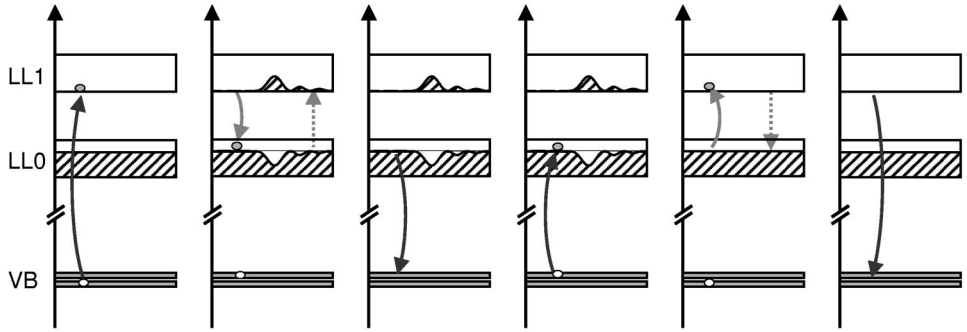

FIG. 16. Magnetoplasmon correlation (MPC) contribution to the FWM signal. The first three panels describe the Stokes Raman scattering process for the creation of a MP excitation. The reverse, anti-Stokes Raman process, which returns the system to the ground state, is shown in the final three panels. Note the similarity of this process and coherent anti-Stokes Raman scattering with phonons.

excitations described by $\overline{P^L}(t)$. At resonance, $\omega=\overline{\Omega}$, this energy dependence manifests itself as a large increase in the imaginary part of the magetoexciton energy, or a large increase in the dephasing. Since $\overline{\Omega}\sim\Omega_1$, this leads to the increase in linewidth for LL1 observed in the linear absorption measurements. This effect is exacerbated when we consider higher orders in the applied field.

At second order in the electric field, we must consider the interactions between two photoexcited pairs, and also influence of the excited electron gas configurations. We approximate the *X*-*X* interactions at the mean-field HF level. There is therefore only one second-order equation necessary for our model, the equation for the magnetoplasmon correlation function $\mathcal{M}(t)$,

$$i\partial_t\mathcal{M}(t)=(\Omega_M-i\gamma_M)\mathcal{M}(t)+[P_1^L{}^*(t)-P_0^L{}^*(t)][P_1^L(t)-P_0^L(t)]. \quad (8)$$

This correlation function describes the intermediate MP state. The driving term of Eq. (8) is similar to a coherent density, $\propto|P^L|^2$, and describes the creation of a MP excitation from the photoexcited *X* states. The time dependence of $\mathcal{M}(t)$, which is found from the integration of this equation, will lead to additional non-Markovian effects in the dynamics of the nonlinear polarization.

Finally we can write the equations of motion for the third-order nonlinear polarization, which gives the FWM signal:

$$\begin{aligned} i\partial_t P_0(t)=&(\Omega_0-i\Gamma_0)P_0(t)-V_{01}P_1(t)-W\overline{P}(t)\\ &+\frac{2\mu\mathcal{E}(t)}{\sqrt{N_0}}P_0^L(t)P_0^L{}^*(t)\\ &+2V_{01}[P_1^L{}^*(t)-P_0^L{}^*(t)]P_1^L(t)P_0^L(t)\\ &-W_M\mathcal{M}^*(t)[P_1^L(t)-P_0^L(t)], \end{aligned} \quad (9)$$

describes the LL0 nonlinear polarization $P_0(t)$. Let us discuss the meaning of the source terms in this equation before presenting the other third-order equations.

The first line of Eq. (9) contains, as in the linear case of Eq. (2), the energy and damping for the oscillation of the LL0 polarization, as well as the coupling between the LL's, $V_{01}P_1(t)$, and the $\overline{P}(t)$ term, which describes the additional dephasing from the $X\leftrightarrow Y$ scattering.

The second and third lines of Eq. (9) give the driving terms for $P_0(t)$, which are similar to the undoped HF theory of Ref. 27. The term of the second line is the familiar Pauli blocking nonlinearity (PB), which exists even in atomic systems, and comes from the fact that the excitations obey the Pauli exclusion principle. It is proportional to the coherent density $|P_n^L(t)|^2$, and can be thought of as the scattering of a laser photon with the coherent density of photoexcited carriers. The third line is the nonlinearity due to the HF *X*-*X* interactions. Similar to the Pauli blocking term above, we can describe this term as the scattering of the photoexcited polarization with the coherent density of photoexcited carriers. We refer to this nonlinearity as the bare Coulomb interaction (BCI). While these effects are found in the HF model of FWM in undoped semiconductors, the additional dephasing and screening from the 2DEG will lead to a qualitative difference in the FWM spectrum.

The fourth line of Eq. (9) describes effects that are entirely absent in the undoped case and come from the 2DEG excitations. The parameter W_M gives the strength of the MP correlation contribution to the FWM signal. This source term, which describes the MP correlations (MPC), comes from photoexcitation and time evolution of the MP state, described by $\mathcal{M}(t)$. It describes processes such as the following, shown schematically in Fig. 16. A photoexcited *X* decays into a *Y*, or $\{X\text{-MP}\}$ excitation. The *e*-*h* pair in this state recombines, leading to coherent emission, which leaves the 2DEG in an excited state. This MP propagates in time and then interacts with the second photoexcited *X* into a new *X* state, which is subsequently annihilated by the optical field. It is interesting to note the similarity of this process and the familiar one of coherent anti-Stokes Raman scattering[35] that, however, involves phonons. This process will contribute the FWM signal with a new time dependence, which comes from the equation of motion for $\mathcal{M}(t)$.

The equation of motion for $P_1(t)$ contains similar source terms,

$$\begin{aligned} i\partial_t P_1(t)=&(\Omega_1-i\Gamma_1)P_1(t)-V_{10}P_0(t)+W\overline{P}(t)\\ &+\frac{2\mu\mathcal{E}(t)}{\sqrt{N_1}}P_1^L(t)P_1^L{}^*(t)-2V_{01}[P_1^L{}^*(t)\\ &-P_0^L{}^*(t)]P_1^L(t)P_0^L(t)+W_M\mathcal{M}^*(t)[P_1^L(t)\\ &-P_0^L(t)], \end{aligned} \quad (10)$$

and is of course coupled to $P_0(t)$ by the LL coupling V_{01}. Both $P_0(t)$ and $P_1(t)$ are coupled to $\overline{P}(t)$, which describes

the dephasing of the nonlinear polarization due to the $X \leftrightarrow Y$ scattering, as discussed above for the linear polarization. This serves to reinforce the dephasing induced by this scattering, as well as introduce time-dependent corrections to the coupling. The full equation of motion for $\overline{P}(t)$ contains many driving terms that come from the interactions among the 2DEG* excited states. However, all of these terms, proportional to $\overline{P^L}(t)$, are damped by an additional dephasing width γ, and thus lead to a broad incoherent contribution to the FWM spectrum. We will neglect all of these terms, and keep only the source terms that describe the coupling to the X states. The equation of motion for $\overline{P}(t)$ is then

$$i\partial_t \overline{P}(t) = (\overline{\Omega} - i\gamma)\overline{P}(t) + [P_1(t) - P_0(t)]. \qquad (11)$$

This equation is very similar to the equation of motion for the linear correlation function $\overline{P^L}(t)$, except it is driven by the nonlinear polarizations $P_1(t) - P_0(t)$. It is interesting to note that the driving terms for many of these model equations [see Eqs. (4) and (8)–(11)] are proportional to the quantity $P_1^L(t) - P_0^L(t)$ or $P_1(t) - P_0(t)$. This shows clearly that the correlations considered here are driven by the difference between the excitation of LL1 and LL0. The energy of this induced polarization is the difference in LL energies, which is nearly resonant with the MP energy, leading to our enhanced correlation effects and non-Markovian time dependence.

We can solve these model equations and compare the results to the experimental data shown above. We start by assuming a laser excitation of the form $\mathcal{E}(t) = e^{i\vec{k}_2 \cdot \vec{r}}\mathcal{E}_p(t) + e^{i\vec{k}_1 \cdot \vec{r}}\mathcal{E}_p(t + \Delta t)$, where $\mathcal{E}_p(t)$ is the Gaussian envelope of the pulses emitted by the laser. We then solve the equations above as a function of time t and time delay Δt, keeping only the terms leading to a nonlinear signal in the $2\vec{k}_2 - \vec{k}_1$ direction, and perform a Fourier transform of the nonlinear polarization to get $P(\Delta t, \omega)$. The FWM signal measured in our experiments is $S_{\mathrm{SR}}(\Delta t, \omega) \propto |P(\Delta t, \omega)|^2$.

By fitting the calculated linear polarization spectrum to the linear absorption measurements taken to characterize our sample, we can fix the parameters V_{01} and W, and the dephasing parameters Γ_n and γ, to within $\pm 50\%$. This is shown in Fig. 17, which compares the calculated absorption $\alpha(\omega) \propto \mathrm{Im}\{\chi^{(1)}(\omega)\} = \mathrm{Im}\{P^L(\omega)/\mathcal{E}(\omega)\}$ with our measured absorption spectra for the MDQW sample at $B = 8$ T. The fit is quite good overall, giving the correct ratio of peak heights and widths. Recall that the valence band structure of the sample leads to additional peaks in the spectrum, which we do not include in our model. This gives the small peak just above the LL0 energy. Varying the parameters within the fitting range ($\pm 50\%$) yields is no significant change to the calculated FWM signal. Essentially, this leaves us with two free parameters in the calculation of the nonlinear polarization, the strength of the MPC term, W_M, and the MP energy Ω_M.

The simulated FWM signal with the optimal choice of parameters, $S_{\mathrm{SR}}^{\mathrm{model}}(\Delta t, \omega)$ is presented in Fig. 18, along with the experimental results $S_{\mathrm{SR}}^{\mathrm{doped}}(\Delta t, \omega)$, for the case where we excite the two LL's equally. As the figure clearly shows, the simulations are able to recreate both the transfer of signal strength to LL0 and the pronounced beats coming from only the single level. The beat period in the simulation is given by the inverse of the LL energy difference, as in the experiment.

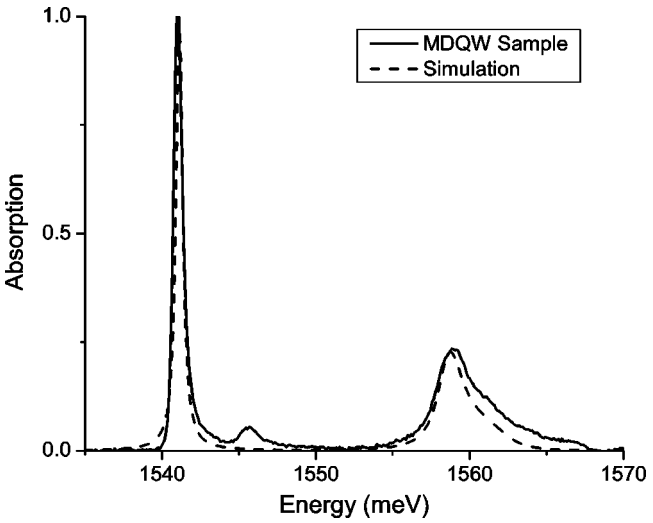

FIG. 17. Simulation of the linear absorption spectrum. We fit the linear polarization calculated from the model (dashed curve) to the MDQW sample absorption spectrum (solid curve). This fit is for $V_{01} = 0.5$ meV, $W = 3.4$ meV^2, and $\gamma = 2.7$ meV. The fit is quite good in terms of the ratio of oscillator strength and peak width.

When we move the laser to excite only into LL1, we can also recreate the transfer of signal strength, as shown in Fig.

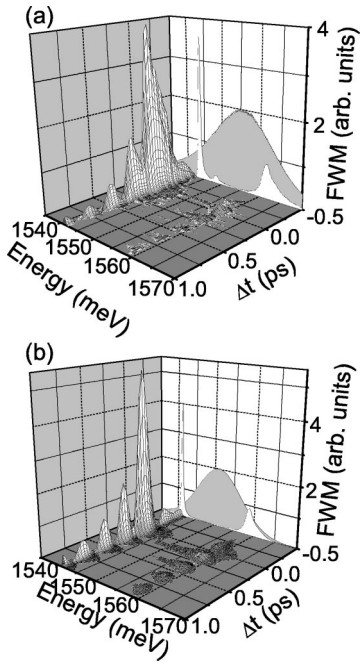

FIG. 18. Simulation of the FWM signal for excitation of both LL's equally. (a) The signal from the MDQW sample for $B = 8$ T, when we excite an equal number of *e-h* pairs into both LL0 and LL1 [same as Fig. 6(a)]. (b) The simulated signal $S_{\mathrm{SR}}^{\mathrm{model}}(\Delta t, \omega)$ for the same conditions as (a). The laser pulse and absorption spectra are projected on the back screen.

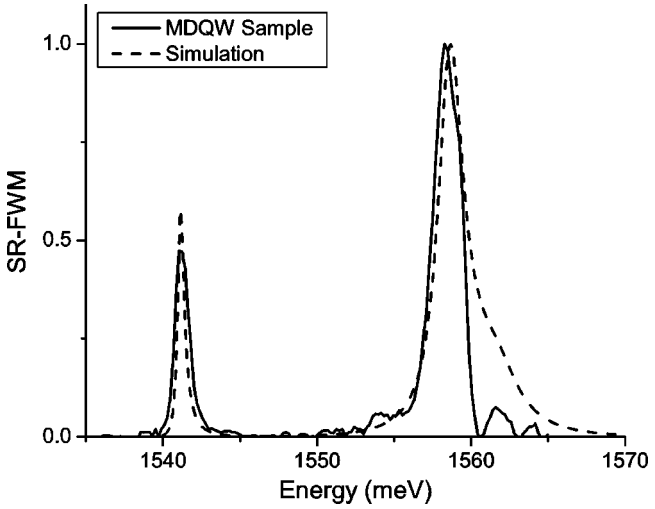

FIG. 19. Simulation of the FWM signal at $\Delta t=0$ for the preferential excitation of LL1. The black line shows the signal from the MDQW sample for $B=8$ T, at $\Delta t=0$, when we excite LL1 preferentially (60:1 excitation of LL1:LL0, same as Fig. 8), and the simulation for the same excitation is shown in the dashed line. The enhancement of the LL0 signal in the simulations is given by $R^{\text{model}}=19.8$, within 15% of the experimental value.

19. Again the signal from LL0 is greatly enhanced relative to LL1, just as in the experiment. Recall that for the experiments we calculated the relative emission ratio R, which gives an estimate for the amount of LL0 enhancement relative to the excitation density [see Eq. (1)]. For the MDQW sample and this excitation condition, we found $R^{\text{doped}}=17.5$, where $R=1$ corresponds to a ''normal'' response. For the simulations we find $R^{\text{model}}=19.8$, which is within 15% of the experimental value.

The model is able to describe the time dependence of this signal as well. Recall that for excitation of LL1, the LL0 signal had a very large $\Delta t<0$ signal, so that the signal was almost symmetric as a function of time delay. In Fig. 20 we show $S_{\text{SR}}^{\text{model}}(\Delta t)$ at the LL0 and LL1 emission energies, compared to the experimental results. The $\Delta t<0$ signal is much larger from LL0 than from LL1, as in the experiment. This behavior can be traced to the non-Markovian dephasing of the polarization and the enhanced LL1 dephasing due to the $X\rightarrow Y$ scattering.

V. CONCLUSION

In conclusion, we have shown that the presence of the 2DEG in a MDQW sample leads to a time-dependent Coulomb coupling of the photoexcited carriers that cannot be treated using the conventional theories for understanding correlations in undoped semiconductors. We have shown that the increased scattering of higher LL carriers with the 2DEG leads to an increase in dephasing and non-Markovian effects that can be seen even in the linear optical response. The FWM results show a strong inter-LL coupling with an unusual time dependence due to the propagation in time of long-lived MP excitations and their interactions with the photoexcited carriers.

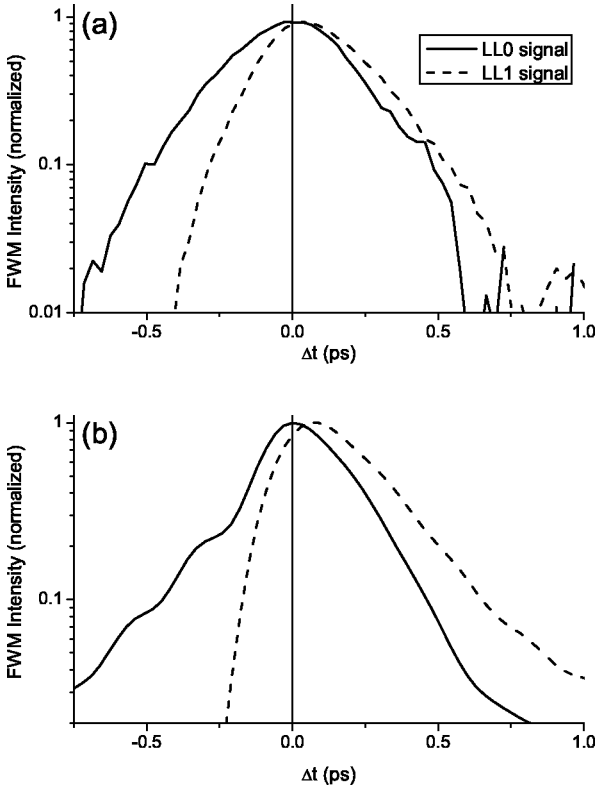

FIG. 20. Simulation of the FWM signal as a function of Δt for the preferential excitation of LL1. The experimental results are shown in (a), for the MDQW sample for $B=8$ T, when we excite LL1 preferentially (60:1 excitation of LL1:LL0, same as Fig. 9), at the LL0 emission energy (solid curve) and the LL1 emission energy (dashed curve). The simulated data is shown in (b) for the same conditions. The signals have been normalized for clarity. Notice the large negative delay signal from the LL0 signal.

ACKNOWLEDGMENTS

We would like to thank T.V. Shahbazyan for many useful discussions. The work was supported by the U.S. DOE, under Contract No. DE-AC03-76SF00098 (Berkeley), and by U.S. DOE, Grant No. DE-FG02-01ER45916, the NSF, and ONR-DARPA/SPINS (I.E.P.).

[1] See, for example, D. S. Chemla and J. Shah, Nature (London) **411**, 549 (2001) and references therein.

[2] D. S. Chemla, in *Nonlinear Optics in Semiconductors*, edited by E. Garmire and A. Kost (Academic Press, San Diego, 1999), Vol. 58, p. 175, and references therein.

[3] J. Shah, *Ultrafast spectroscopy of semiconductors and semiconductor nanostructures* (Springer Verlag, Berlin; New York, 1999).

[4] S. Mukamel, *Principles of nonlinear optical spectroscopy* (Oxford University Press, New York, 1995).
[5] P. Kner, S. Bar-Ad, M. V. Marquezini, D. S. Chemla, R. Lovenich, and W. Schafer, Phys. Rev. B **60**, 4731 (1999); G. Bartels, A. Stahl, V. M. Axt, B. Haase, U. Neukirch, and J. Gutowski, Phys. Rev. Lett. **81**, 5880 (1998); V. M. Axt, S. R. Bolton, U. Neukirch, L. J. Sham, and D. S. Chemla, Phys. Rev. B **63**, 115303 (2001), and references therein.
[6] M. Wegener and D. S. Chemla, Chem. Phys. **251**, 269 (2000).
[7] H. Haug and A.-P. Jauho, *Quantum kinetics in transport and optics of semiconductors* (Springer, Berlin; New York, 1996).
[8] H. Haug and S. W. Koch, *Quantum Theory of the Optical and Electronic Properties of Semiconductors*, 2nd ed. (World Scientific, Singapore, 1993).
[9] S. G. Louie, in *Topics in Computational Materials Sciences*, edited by C. Y. Fong (World Scientific, Singapore, 1977), p. 96.
[10] L. J. Sham, Phys. Rev. **150**, 720 (1966).
[11] See, for example, V. M. Axt and S. Mukamel, Rev. Mod. Phys. **70**, 145 (1998), and references therein.
[12] I. Balslev and E. Hanamura, Solid State Commun. **72**, 843 (1989).
[13] V. M. Axt and A. Stahl, Z. Phys. B: Condens. Matter **93**, 195 (1994); **93**, 205 (1994); K. Victor, V. M. Axt, and A. Stahl, Phys. Rev. B **51**, 14 164 (1995).
[14] W. Schäfer, D. S. Kim, J. Shah, T. C. Damen, J. E. Cunningham, K. W. Goosen, L. N. Pfeiffer, and K. Kohler, Phys. Rev. B **53**, 16 429 (1996).
[15] Q. T. Vu, H. Haug, W. A. Hügel, S. Chatterjee, and M. Wegener, Phys. Rev. Lett. **85**, 3508 (2000).
[16] I. E. Perakis and D. S. Chemla, Phys. Rev. Lett. **72**, 3202 (1994); T. V. Shahbazyan, N. Primozich, I. E. Perakis, and D. S. Chemla, *ibid.* **84**, 2006 (2000); N. Primozich, T. V. Shahbazyan, I. E. Perakis, and D. S. Chemla, Phys. Rev. B **61**, 2041 (2000).
[17] I. E. Perakis and T. V. Shahbazyan, Surf. Sci. Rep. **40**, 1 (2000).
[18] N. Primozich, T. V. Shahbazyan, I. E. Perakis, and D. S. Chemla, Phys. Rev. B **61**, 2041 (2000).
[19] T. V. Shahbazyan, N. Primozich, I. E. Perakis, and D. S. Chemla, Phys. Rev. Lett. **84**, 2006 (2000).
[20] D. Heiman, B. B. Goldberg, A. Pinczuk, C. W. Tu, A. C. Gossard, and J. H. English, Phys. Rev. Lett. **61**, 605 (1988).
[21] T. Uenoyama and L. J. Sham, Phys. Rev. B **39**, 11 044 (1989).
[22] *Perspectives in Quantum Hall Effects*, edited by Das Sarma and A. Pinczuk (Wiley, New York, 1997).
[23] H. L. Stormer, D. C. Tsui, and A. C. Gossard, Rev. Mod. Phys. **71**, S298 (1999).
[24] See, for example, *Perspectives in Quantum Hall Effects*, edited by Das Sarma and A. Pinczuk (Wiley, New York, 1997); H. L. Stormer, D. C. Tsui, and A. C. Gossard, Rev. Mod. Phys. **71**, S298 (1999).
[25] See, for example, I. V. Kukushkin, R. J. Haug, K. von Klitzing, and K. Ploog, Phys. Rev. Lett. **72**, 736 (1994); B. B. Goldberg, D. Heiman, A. Pinczuk, L. Pfeiffer, and K. West, *ibid.* **65**, 641 (1990); E. H. Aifer, B. B. Goldberg, and D. A. Broido, *ibid.* **76**, 680 (1996).
[26] N. A. Fromer, C. Schuller, D. S. Chemla, T. V. Shahbazyan, I. E. Perakis, K. Maranowski, and A. C. Gossard, Phys. Rev. Lett. **83**, 4646 (1999).
[27] C. Stafford, S. Schmitt-Rink, and W. Schaefer, Phys. Rev. B **41**, 10 000 (1990).
[28] N. A. Fromer, C. E. Lai, D. S. Chemla, I. E. Perakis, D. Driscoll, and A. C. Gossard, Phys. Rev. Lett. **89**, 067401 (2002).
[29] C. Kallin and B. I. Halperin, Phys. Rev. B **30**, 5655 (1984).
[30] A. H. Macdonald, J. Phys. C **18**, 1003 (1985).
[31] A. H. Macdonald, H. C. A. Oji, and S. M. Girvin, Phys. Rev. Lett. **55**, 2208 (1985).
[32] D. A. Broido and L. J. Sham, Phys. Rev. B **31**, 888 (1985).
[33] S. R. E. Yang, D. A. Broido, and L. J. Sham, Phys. Rev. B **32**, 6630 (1985).
[34] S. R. E. Yang and L. J. Sham, Phys. Rev. Lett. **58**, 2598 (1987).
[35] M. Levenson, *Introduction to Nonlinear Laser Spectroscopy* (Academic Press, New York, 1982).
[36] A. Karathanos, I. E. Perakis, N. A. Fromer, and D. S. Chemla (unpublished).
[37] N. A. Fromer, P. Kner, D. S. Chemla, R. Lovenich, and W. Schafer, Phys. Rev. B **62**, 2516 (2000).